

# Quantum Feasibility Labeling for NP-complete Vertex Coloring Problem

Junpeng Zhan<sup>1</sup>

**Abstract:** Many important science and engineering problems can be converted into NP-complete problems which are of significant importance in computer science and mathematics. Currently, neither existing classical nor quantum algorithms can solve these problems in polynomial time. To address this difficulty, this paper proposes a quantum feasibility labeling (QFL) algorithm to label all possible solutions to the vertex coloring problem, which is a well-known NP-complete problem. The QFL algorithm converts the vertex coloring problem into the problem of searching an unstructured database where good and bad elements are labeled. The recently proposed variational quantum search (VQS) algorithm was demonstrated to achieve an exponential speedup, in circuit depth, up to 26 qubits in finding good element(s) from an unstructured database. Using the labels and the associated possible solutions as input, the VQS can find all feasible solutions to the vertex coloring problem. The number of qubits and the circuit depth required by the QFL each is a polynomial function of the number of vertices, the number of edges, and the number of colors of a vertex coloring problem. We have implemented the QFL on an IBM Qiskit simulator to solve a 4-colorable 4-vertex 3-edge coloring problem.

**Keywords:** NP-complete problem, quantum algorithm, unstructured database, variational quantum search, vertex coloring problem

## 1. Introduction

NP-complete problems [1], [2] are a type of problem for which it is believed that there is no efficient algorithm for solving them. Many science and engineering problems can be converted into NP-complete problems. These problems are typically characterized by the need to find the optimal solution among a large number of possible solutions.

Here are a few examples of the many science and engineering problems that can be converted into NP-complete problems: Traveling Salesman Problem [3]–[5] (of interest in transportation and logistics), Knapsack Problem [6]–[9] (of interest in resource allocation and inventory management), Satisfiability Problem [10]–[14] (SAT, of interest in computer science, artificial intelligence, and logic), Subset Sum Problem [1] (of interest in cryptography and computer security), Graph Coloring Problem [15], [16] (of interest in scheduling and resource allocation), Hamiltonian Cycle Problem [15]–[17] (of interest in network design), and the Steiner Tree Problem [17] (of interest in telecommunications and computer networks).

Despite the many efforts [3]–[17] to develop classical algorithms for solving NP-complete problems, it is generally believed that there is no classical algorithm that can solve NP-complete problems in polynomial time, which means that the time and resources required to solve these problems increase faster than a polynomial function of the size of the problem. Whether NP-complete problems can be solved efficiently is an extremely important but unsolved question. The Clay Mathematics Institute has offered a prize of \$1 million for a solution to the problem.

Quantum computing has been the subject of intense research and development in recent years due to its potential to solve certain types of problems much faster than classical computers [18]–[29]. The progress in quantum computer hardware development has been particularly impressive in recent years. Researchers have made significant advances in the design and construction of quantum computer hardware [27], [28], [30]–[33], and several companies have released

---

<sup>1</sup> Department of Renewable Energy Engineering, Alfred University, Alfred, NY, USA. E-mail: zhanj@alfred.edu

commercial quantum computers that are available for use by researchers and businesses [34]–[36]. These quantum computers have demonstrated impressive performance on a variety of tasks [18], [27], [28], and their capabilities are expected to continue to improve in the coming years [37], [38].

In addition to the progress in quantum computer hardware development, there has also been significant progress in the development of a wide range of quantum algorithms for a variety of different types of problems [20], [21], [29], [39]–[49]. Some of these algorithms have demonstrated impressive performance on tasks that are difficult or impossible to solve using classical algorithms [18], [27], and it is expected that the development of quantum algorithms will continue to be an active area of research in the coming years.

Depending on whether classical computers are used, we can divide quantum algorithms into 1) pure quantum algorithms such as Shor's algorithm for factorization [24] and Grover's algorithm for searching unordered lists [22], [23], and 2) variational quantum algorithms (VQAs) [50]–[52] which involve both classical and quantum computers. VQAs have been successfully used in areas such as optimization problems [53]–[55], quantum chemistry [32], [50], [52], [56], [57], and machine learning [42], [58]–[63], and are expected to help achieve systematic quantum supremacy over classical algorithms using hundreds of qubits which are already available [34].

Given the promising potential and recent success of quantum computing, it is natural to ask whether it can provide a quantum exponential speedup in solving NP-complete problems. *Unfortunately, it is widely believed (though not proven) that the answer is no* [64], [65]. However, a recent paper [29] proposed a variational quantum search (VQS) algorithm, which has been shown to have an exponential advantage, in the circuit depth, over Grover's search algorithm in searching an unstructured database, up to a limit of 26 qubits (the limit is due to the memory constraints of the 48-GB GPU used in the calculation). According to paper [29], a depth-10 quantum circuit can amplify the total probability of  $k$  ( $k \geq 1$ ) good elements, out of  $2^n$  elements represented by  $n+1$  qubits, from  $k/2^n$  to nearly 1 for  $n$  up to 26. Additionally, the maximum depth of quantum circuits in the VQS increases linearly with the number of qubits. Given that Grover's algorithm can provide quadratic speedup in solving NP-complete problems, the VQS could solve these problems in polynomial time for up to 26 qubits. However, for larger instances beyond 26 qubits, the efficiency of VQS needs further in-depth exploration and investigation.

This paper focuses on the vertex coloring problem [15], [16] which is a well-known NP-complete problem in graph theory. It involves assigning colors to the vertices of a graph (Fig. 1 shows a graph with 7 vertices) such that no two adjacent vertices have the same color. It has many practical applications, including scheduling, resource allocation, and network design, and has been the subject of much research in both classical and quantum computing. Note that solving one NP-complete is equivalent to solving all hundreds of NP-complete problems.

The **Vertex Coloring problem** entails a set of constraints: within a graph, no two directly connected vertices should share the same color. In this context, a solution within an  $n$ -vertex graph is presented as a vector comprising  $n$  elements, where each element corresponds to a color associated with a specific vertex in the graph. A solution is deemed *feasible* when it satisfies all constraints, ensuring that no two adjacent vertices share the same color. Conversely, a solution is classified as *infeasible* if it violates at least one of these constraints.

Paper [66] proposed a quantum method that has a complexity of  $O(1.9140^n)$  in solving a  $k$ -colorable  $n$ -vertex graph coloring problem. Paper [67] presented a simple method based on Grover's algorithm to obtain a quadratic speedup in solving NP-complete problems.

To solve the vertex coloring problem more efficiently, this paper proposes a quantum feasibility labeling (QFL) algorithm, which assigns a feasibility label to every possible feasible/infeasible solution. By using the labels and the associated solutions as input, the VQS can then be directly used to find the feasible solutions in polynomial time. If the VQS is proven to be

efficient for more than 26 qubits [29], the combination of the QFL and VQS will be the first quantum algorithm to solve an NP-complete problem in polynomial time.

Section 2 describes the QFL algorithm. Section 3 explains how to use VQS to find the feasible solutions to the vertex coloring problem. Results are presented in Section 4 followed by conclusions given in Section 5.

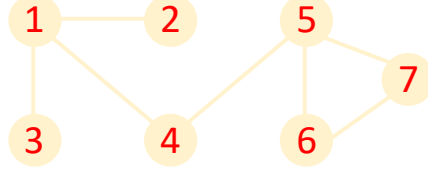


Fig. 1. A graph with 7 vertices and 7 edges. A line between two vertices indicates the two vertices are directly connected, and we also say that the two vertices are adjacent.

## 2. Quantum Feasibility Labeling Algorithm

In this section, we detail the QFL algorithm. The section is structured as follows. Subsections 2.1 and 2.2 describe two pivotal components within the QFL: the SO/SOR module and the reset circuit, respectively. Subsection 2.3 offers a comprehensive overview of the entire quantum circuit employed in the QFL and describes the steps to construct the circuit for the QFL. Subsections 2.4 and 2.5 expand on the quantum subtraction and quantum OR circuit, illustrating their extension to accommodate additional qubits. Finally, in Subsection 2.6, we conduct a detailed complexity analysis for the QFL.

The QFL generates a feasibility label for each solution. The *feasibility label* is represented by a single qubit which is in either  $|0\rangle$  or  $|1\rangle$  state, indicating that the solution is infeasible or feasible, respectively. The number of *data qubits* is set to the product of the number of vertices and the number of qubits per vertex.

The number of possible colors for a vertex is  $k$ . Then, the total number of possible solutions to the vertex coloring with  $n$  vertices is equal to  $k^n$ . Let  $m$  represent the minimal integer number such that  $2^m \geq k$ . Then  $m \times n$  qubits represent  $2^{mn}$  states which can represent all the  $k^n$  solutions as  $2^{mn} \geq k^n$ . Therefore, a circuit of  $m \times n$  qubits is used to represent all the possible solutions. The QFL uses a single qubit to represent the feasibility label of all possible solutions, which is possible because  $2^{m(n+1)} \geq k^n + k^n$ , i.e., adding one more qubit can represent the feasibility label for every possible solution.

Note that each color is uniquely represented by a unique value of a state. Take  $m=2$  for example, a 2-qubit state has four possible measurement values (i.e.,  $|00\rangle$ ,  $|01\rangle$ ,  $|10\rangle$ , and  $|11\rangle$ ) and we can let them represent four different colors, respectively.

### 2.1 Quantum SO/SOR Module

Before delving into the QFL, we detail its core module, SO/SOR. First, a *quantum subtraction circuit* compares two groups of  $m$ -qubit data (the blue part of Fig. 2 shows an example with  $m=2$ ). The output of quantum subtraction is stored in  $m+1$  *Ancilla qubits*. This can be described as Eq. (1):

$$|\mathbf{a}, \mathbf{b}, \mathbf{0}, 0\rangle \rightarrow |\mathbf{a}, \mathbf{b}, \mathbf{a} - \mathbf{b}, 0\rangle \quad (1)$$

where a notation in bold indicate that it involves multiple qubits.

Then, a *quantum OR circuit* (the pink part of Fig. 2 shows an example with three input qubits and one output qubit) obtains a one-qubit *feasibility label* based on the subtraction results. This can be described as Eq. (2):

$$|\mathbf{a}, \mathbf{b}, \mathbf{a} - \mathbf{b}, 0\rangle \rightarrow |\mathbf{a}, \mathbf{b}, \mathbf{a} - \mathbf{b}, d\rangle \quad (2)$$

where  $d$  represents the logical OR result for every bit in  $\mathbf{a} - \mathbf{b}$ , which can be described as Eq. (3):

$$d = (a - b)_1|(a - b)_2|\cdots|(a - b)_m|(a - b)_{m+1} \quad (3)$$

where  $(a - b)_i$ ,  $i = 1, 2, \dots, m, m + 1$ , represent the  $i$ th bit of  $\mathbf{a} - \mathbf{b}$ .

At last, a **reset circuit** (an example for the 2-qubit subtraction [68] and 3-input OR module is shown in Fig. 3) resets the state of each Ancilla qubit to  $|0\rangle$  such that every subtraction can use the same Ancilla qubits without requesting new qubits. This can be described as Eq. (4):

$$|\mathbf{a}, \mathbf{b}, \mathbf{a} - \mathbf{b}, d\rangle \rightarrow |\mathbf{a}, \mathbf{b}, \mathbf{0}, d\rangle \quad (4)$$

For the convenience of expression, the quantum subtraction and quantum OR circuits are collectively referred to as an **SO module**. The SO module and the reset circuit are collectively referred to as an **SOR module**. Fig. 2 shows an SOR module with data input on the far left.

To better understand the SO module, Table 1 provides its truth table. Note that the subtraction circuit does not change the states of input data, which can be easily verified from Figs. 2 and 5. From Table 1, we can conclude that output  $o_7 = 0$  when  $q_3q_2$  is equal to  $q_1q_0$  and  $o_7 = 1$  when  $q_3q_2$  is different from  $q_1q_0$ . This is what we need, i.e., the feasibility label is 1 when the colors of two directly connected vertices are different and 0 otherwise.

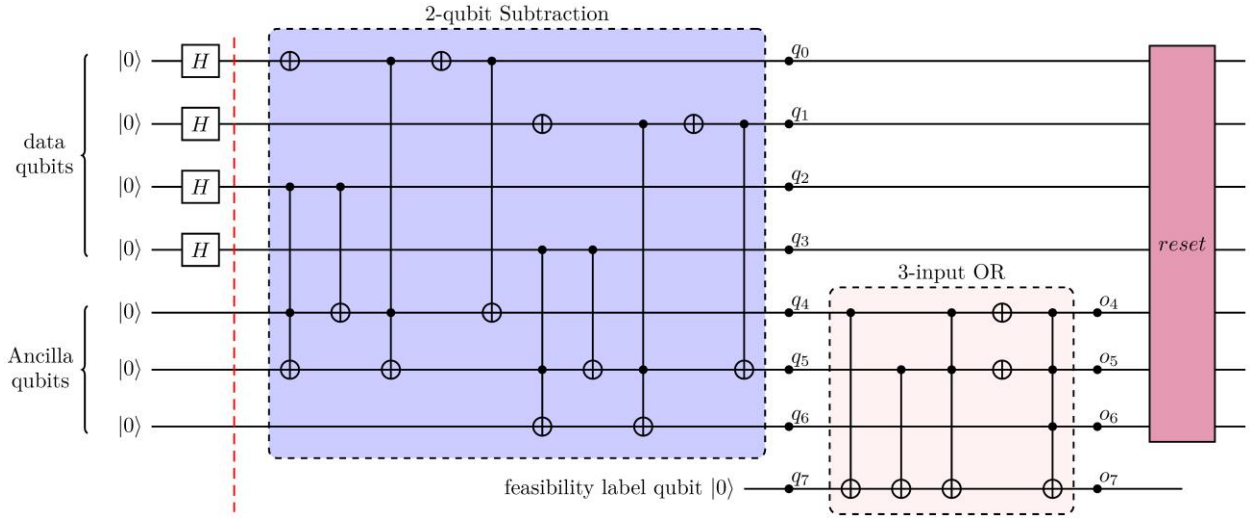


Fig. 2. Data input (left-hand side of the red dashed line) and an SOR module (right-hand side of the red dashed line) consisting of a 2-qubit subtraction, a 3-input OR, and a reset circuit.

**Table 1.** The truth table for the circuit given in Fig. 2, where  $o_7 = q_6|q_5|q_4$  and  $q_6q_5q_4 = q_1q_0 - q_3q_2$ . Note:  $o_6 = q_6$ ,  $o_5 = \overline{q_5}$ ,  $o_4 = \overline{q_4}$ , where the quantum states given in the top row of the table are indicated in Fig. 2 (on the right-hand sides of the blue and pink blocks).

row	$o_7$	$o_6$	$o_5$	$o_4$	$q_6$	$q_5$	$q_4$	$q_3$	$q_2$	$q_1$	$q_0$
1	0	0	1	1	0	0	0	0	0	0	0
2	0	0	1	1	0	0	0	0	1	0	1
3	0	0	1	1	0	0	0	1	0	1	0
4	0	0	1	1	0	0	0	1	1	1	1
5	1	0	0	0	0	1	1	0	0	1	1
6	1	0	0	1	0	1	0	0	0	1	0
7	1	0	0	1	0	1	0	0	1	1	1
8	1	0	1	0	0	0	1	0	0	0	1
9	1	0	1	0	0	0	1	0	1	1	0
10	1	0	1	0	0	0	1	1	0	1	1
11	1	1	0	0	1	1	1	0	1	0	0

12	1	1	0	0	1	1	1	1	0	0	0	1
13	1	1	0	0	1	1	1	1	1	1	1	0
14	1	1	0	1	1	1	0	1	0	0	0	0
15	1	1	0	1	1	1	0	1	1	0	1	1
16	1	1	1	0	1	0	1	1	1	0	0	0

## 2.2 Quantum Reset Circuit

Each  $m$ -qubit SO/SOR module needs  $m+1$  Ancilla qubits that have initial states of  $|0\rangle$ . Here we use a reset circuit to return the state of each Ancilla qubit to  $|0\rangle$  after passing through the SO/SOR module such that the Ancilla qubits can be reused for the next SO/SOR module. The basic idea is to use multi-controlled multi-target CNOT to change the state of each Ancilla qubit to  $|0\rangle$  according to the relationship between the input data and the output of the OR circuit. For example, for the circuit given in Fig. 2, the relationship (or truth table) between  $o_4-o_6$  and  $q_0-q_3$  is given in Table 1. We can then use the values of  $q_0-q_3$  as controls and let the qubits associated with  $o_4-o_6$  be the target(s) if they are in state  $|1\rangle$ , which can reset the outputs of  $o_4-o_6$  to  $|0\rangle$ . Fig. 3 provides an example reset circuit for the reset block (rightmost, in red) in Fig. 2. Fig. 3 has 15 layers, each associated with a row in Table 1. Note that row 5 of Table 1 does not need a layer in Fig. 3 because its  $o_4-o_6$  are already in state  $|0\rangle$ .

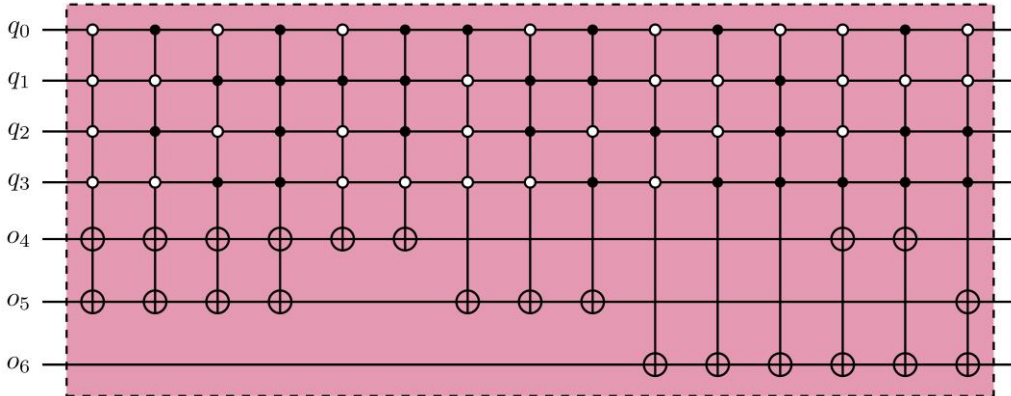


Fig. 3. The reset circuit used in Fig. 2.

## 2.3 Entire Quantum Circuit for Quantum Feasibility Labeling

Each SO/SOR module corresponds to a constraint of the vertex coloring problem. Each SO/SOR module has a one-qubit feasibility label, denoted as  $L_i$  (shown in the lower-right corner of each SO/SOR block in Fig. 4), indicating whether the constraint is feasible or not. All constraints need to be satisfied for a feasible solution. Therefore, we use an AND circuit to combine two SO/SOR together in a sequential way. The feasibility label qubits of the first two SO/SOR modules are the input of the first AND circuit. Starting from the third SO/SOR module, the output of the previous AND circuit is used as the second input of the current AND circuit. According to Eqs. (1)-(4) and by denoting the data input of the  $i$ th SO/SOR module as  $\mathbf{a}_i, \mathbf{b}_i$ , we can represent the  $i$ th SO/SOR module as Eq. (5):

$$|\mathbf{a}_i, \mathbf{b}_i, \mathbf{0}, 0\rangle \rightarrow |\mathbf{a}_i, \mathbf{b}_i, \mathbf{a}_i - \mathbf{b}_i, d_i\rangle \quad (5)$$

where  $d_i \in \{0,1\}$ .

Then the input-output logic for the first AND circuit shown in Fig. 4 can be expressed as Eq. (6):

$$|\mathbf{a}_1, \mathbf{b}_1, \mathbf{0}, \mathbf{a}_2, \mathbf{b}_2, \mathbf{0}, d_1, d_2, 0\rangle \rightarrow |\mathbf{a}_1, \mathbf{b}_1, \mathbf{0}, \mathbf{a}_2, \mathbf{b}_2, \mathbf{0}, d_1, d_2, d_1 \& d_2\rangle \quad (6)$$

where  $d_1$  and  $d_2$  represent the output of the feasibility label qubit of the first and second SO/SOR modules, respectively, and  $d_1 \& d_2$  represents the logic AND of  $d_1$  and  $d_2$ .

Furthermore, the input-output logic for the  $(j-1)$ th AND circuit, which is located at the right-hand-side of the  $j$ th SO/SOR module, can be represented as Eq. (7):

$$|\mathbf{A}, \mathbf{B}, \mathbf{0}, d_j, D_{j-1}, 0\rangle \rightarrow |\mathbf{A}, \mathbf{B}, \mathbf{0}, d_j, D_{j-1}, D_j\rangle, \quad 3 \leq j \leq g \quad (7)$$

where  $\mathbf{A}, \mathbf{B}, \mathbf{0}$  represent all the data input and state  $|0\rangle$  that is input into all ancillary qubits,  $g$  denotes the number of edges in the coloring problem,  $d_j$  represents the output of the feasibility label qubit of the  $j$ th SO/SOR modules, respectively,  $D_{j-1}$  represents  $d_1 \& d_2 \& \dots \& d_{j-1}$ ,  $j \geq 3$ , and  $D_j$  represents  $D_{j-1} \& d_j$  which can be expanded into  $D_j = d_1 \& d_2 \& \dots \& d_{j-1} \& d_j$ . For a  $g$ -edge coloring problem, there are  $g$  SO/SOR module and, therefore, the maximum value of  $j$  is  $g$ .

For the data input, each vertex has  $m$  qubits. If a vertex is involved in multiple SO/SOR blocks, all blocks should use the same  $m$  qubits for that vertex, which is possible because the states of the data qubits do not change before and after the SO/SOR block. Also, the reset circuit does not change the state of any data qubits.

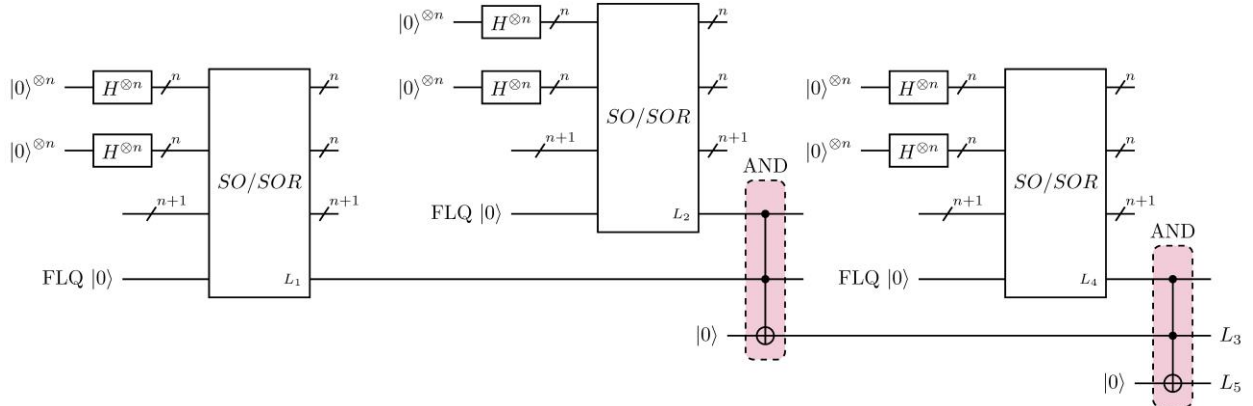


Fig. 4. The quantum circuit for the Quantum Feasibility Labeling algorithm, where FLQ is short for feasibility label qubit.

We describe the construction of the entire circuit of QFL in the following 4 steps.

**Step 1 - Feasibility label:** Use two SO/SOR modules (see the left and middle parts of Fig. 4) to obtain two feasibility labels (i.e.,  $L_1$  and  $L_2$  in Fig. 4) for the first two constraints, respectively.

**Step 2 - Quantum AND:** The two feasibility labels are converted into one feasibility label using a quantum AND circuit (see the red part in the middle of Fig. 4). The output of this circuit is a one-qubit feasibility label ( $L_3$  in Fig. 4). The logical relationship for this AND circuit can be represented as  $L_3=L_1 \& L_2$ .

**Step 3 - Incremental step:** Then, a new SOR circuit (see the right side of Fig. 4) is added for a new constraint of the vertex coloring problem. The output at the feasibility label qubit of this circuit ( $L_4$ ) and the feasibility label ( $L_3$ ) obtained from the previous AND circuit are used as inputs to a new quantum AND circuit (see the rightmost red part of Fig. 4). The output of the new quantum AND circuit is a one-qubit feasibility label ( $L_5$ ). The logical relationship for this circuit can be expressed as  $L_5=L_3 \& L_4$ .

**Step 4 - Repeat the incremental step** for each remaining constraint of the vertex coloring problem.

Now, the feasibility label qubit from the last quantum AND circuit and the data qubits together represent all solutions and their feasibility labels. For an  $n$ -vertex  $g$ -edge coloring problem, there

are  $g$  modules, and the  $D_j$  in Eq. (7), where  $j = g$ , is the feasibility label representing the feasibility of all solutions  $\mathbf{a}_1, \mathbf{b}_1, \mathbf{a}_2, \mathbf{b}_2, \dots, \mathbf{a}_n, \mathbf{b}_n$ .

## 2.4 Quantum Subtraction with More Qubits

This subsection presents the  $m$ -qubit quantum subtraction circuit, shown in Fig. 2 (blue block) and Fig. 5 for  $m=2$  and  $m=3$ , respectively. In Fig. 5, the logical relationship of the 3-qubit quantum subtraction can be expressed as  $q_9q_8q_7q_6 = q_2q_1q_0 - q_5q_4q_3$ . Then, an  $m$ -qubit quantum subtraction circuit can be derived, i.e., connecting  $m$  SUBT blocks in series such that the indices of the four qubits connected to the four wires of a block differ from those of its adjacent block by exactly 1, respectively, where  $m \geq 2$ .

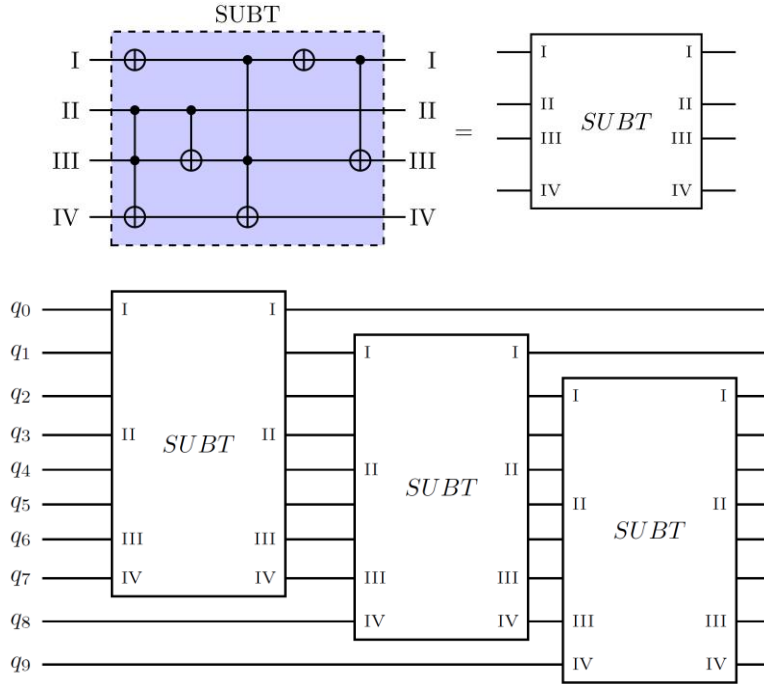


Fig. 5. Quantum subtraction circuits. The top left panel in blue is a 1-qubit quantum subtraction circuit having four qubits indicated by I, II, III, and IV, respectively. Its abstract form (denoted as SUBT) is shown in the top right panel. The bottom panel shows a 3-qubit quantum subtraction circuit consisting of three 1-qubit quantum subtraction circuits. The I, II, III, and IV indicate where the four qubits of a SUBT block are connected to  $q_0$ - $q_9$ . For example, the four qubits of the leftmost SUBT block are connected to  $q_0$ ,  $q_3$ ,  $q_6$ , and  $q_7$ , respectively.

## 2.5 Quantum OR Circuits with More Qubits

This subsection presents the  $m$ -qubit quantum OR circuit, shown in Fig. 2 (pink block) and Fig. 6 for  $m=3$ , and  $m=4$ , respectively. In Fig. 6, the logical relationship of the 4-qubit quantum OR can be expressed as  $q_4 = q_0|q_1|q_2|q_3$ . Then, an  $m$ -input quantum OR circuit can be derived and it can be constructed using the pseudo code given in Algorithm 1.

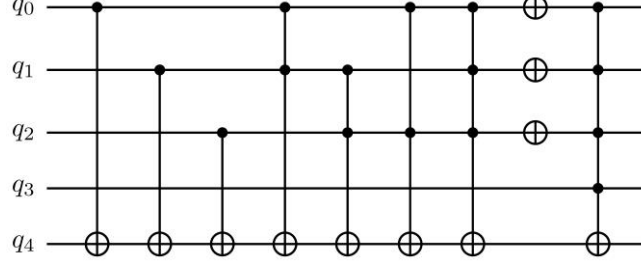


Fig. 6. A 4-input quantum OR circuit.

Algorithm 1. Pseudo code for generating the  $m$ -input quantum OR circuit.

---

**Input:**  $m+1$  qubits  
**Output:**  $m$ -input quantum OR circuit

---

- 1 Add  $m-1$  CNOT gates with the control qubits located at qubits  $q_0 \sim q_{m-2}$ , respectively, and the target qubit for each gate is located at qubit  $q_{m+1}$ .
- 2 Let  $u=2$
- 3 **while**  $u \leq m-1$
- 4     Add a  $C^u(X)$  gate with  $u$  control qubits located at set  $\mathcal{L}$  and a target qubit located at qubit  $q_{m+1}$ .
- 5     Repeat the previous step for  $\mathcal{L}$  being any combinations of  $u$  qubits from  $q_0$  to  $q_{m-2}$ .
- 6      $u \leftarrow u+1$ .
- 7 Add a Pauli X gate to each of qubits  $q_0 \sim q_{m-2}$ .
- 8 Add a  $C^m(X)$  gate with a target qubit located at qubit  $q_{m+1}$  and  $m$  control qubits located at qubits  $q_0 \sim q_{m-1}$ .

---

## 2.6 Complexity Analysis

This subsection calculates the number of qubits and the depth of the circuit required by the QFL for solving a  $k$ -colorable  $n$ -vertex  $g$ -edge coloring problem.

In the calculation given in the following two paragraphs, the reset circuit (the red block on the far right in Fig. 2) is used, i.e., each SO/SOR module in Fig. 4 uses SOR. The total depth of the entire circuit is  $g \left[ 5m + 1 + \left( \sum_{i=1}^m \binom{m}{i} + 2 \right) + (2^{2m} - 1) \right]$ , where the four terms in the square brackets are the depths of the subtraction, AND, OR, and reset circuits, respectively, and  $\binom{m}{i}$  denotes the number of  $i$ -combinations from  $m$  elements. Note that  $\sum_{i=1}^m \binom{m}{i} = 2^m - 1$ . Then, the total depth can be simplified to  $g(2^{2m} + 2^m + 5m + 1)$ . Note that  $m$  is related to the number of possible colors  $k$ , i.e.,  $m = \lceil \log_2 k \rceil$ , where the symbol  $\lceil \cdot \rceil$  means rounding up to the nearest integer number. Then the total depth can be written as  $O(k^2 g)$ .

The total number of qubits is  $mn + (m + 1) + g + (g - 1)$  where the four terms correspond to the numbers of data qubits, Ancilla qubits, feasibility label qubits, output qubits of quantum AND circuits, respectively. It can be simplified as  $mn + m + 2g$ .

In the calculation given in this paragraph, the reset circuit is not used, i.e., each SO/SOR module in Fig. 4 uses SO. The total depth of the entire circuit is  $g \left[ 5m + 1 + \left( \sum_{i=1}^m \binom{m}{i} + 2 \right) \right]$  which can be simplified to  $g[5m + 2^m + 2]$ . Then the total depth can be written as  $O(kg)$ . As the reset circuit is not used, each SO module requires new Ancilla qubits. Therefore, the total number of qubits is  $mn + (m + 1)g + g + (g - 1)$  which can be rewritten as  $mn + (m + 3)g - 1$ .



Table 2 lists the circuit depths and the numbers of qubits in both situations, showing that using the reset circuit reduces the required number of qubits at the expense of deeper circuit depth. When  $k$  (the number of colors) is large, we recommend not using the reset circuit. On the other hand, when  $g$  (the number of edges) is large and  $k$  is small, it is better to use the reset circuit.

Table 2. The circuit depths and the numbers of qubits required by the QFL with and without using the reset circuit for solving a  $k$ -colorable  $n$ -vertex  $g$ -edge coloring problem, where  $m = \lceil \log_2 k \rceil$ .

With Reset Circuit	Circuit Depth	# of qubits
Yes	$O(k^2 g)$	$mn + m + 2g$
No	$O(kg)$	$mn + (m + 3)g - 1$

### 3. Variational Quantum Search

In this section, we discuss how to utilize the VQS to find all feasible solutions to the vertex coloring problem using the output of the QFL as the input to the VQS.

Within the QFL output, there exists a crucial component known as the final labeling qubit, denoted as  $D_j$  in Eq. (7). This qubit assumes a state of  $|1\rangle$  to represent a feasible solution and  $|0\rangle$  to denote an infeasible one. When combined with all possible solutions, this labeling qubit collectively forms an unstructured database. Each element in this database corresponds to a solution, accompanied by its feasibility label. A feasible solution is analogous to a good element, whereas an infeasible solution corresponds to a bad element. This conceptual framework effectively links feasible and infeasible solutions to the concept of an unstructured database. In other words, the QFL algorithm converts the vertex coloring problem into an unstructured database where good elements are labeled with qubit  $|1\rangle$  and bad elements are labeled with qubit  $|0\rangle$ .

Grover's search algorithm (GSA) applies a negative phase to a good element such that the GSA can increase the probability of finding it. In contrast, VQS takes a different approach by attaching a label state,  $|1\rangle$ , to the good elements and  $|0\rangle$  to the bad elements. Both GSA and VQS employ this strategy to amplify the likelihood of identifying the good elements within an unstructured database, as described in [29].

Considering the feasible and infeasible solutions are analogous to good and bad elements within an unstructured database, as described above, VQS can amplify the probability of identifying the feasible solutions. In other words, VQS leverages the label state  $|1\rangle$  on the final labeling qubit to amplify the probability of finding feasible solutions, much like it amplifies the probability of identifying good elements in an unstructured database. Since the QFL algorithm already provides the label qubit, the oracle component in the VQS is not needed when searching the unstructured database generated by the QFL.

### 4. Result

We have implemented the QFL on an IBM Qiskit [34] simulator to solve a 4-colorable 4-vertex 3-edge coloring problem. The three edges are 1-2, 1-3, and 1-4, i.e., vertex 1 connects to vertices 2, 3, and 4, respectively. Based on the principles of permutation and combination, vertex 1 can be colored with any of the four available colors, and then vertices 2, 3, and 4 can each be colored with any of the remaining three colors. As a result, the number of possible feasible solutions is

$4 \times 3 \times 3 \times 3 = 108$ . The circuit used by the QFL is given in Fig. 4, where the three SOR modules are for the three constraints, respectively. These modules use the same qubits for vertex 1, i.e., the output of one SOR block at these qubits is used as input for the next SOR.

The circuit is run and measured 20,000 times with the results shown in Table 3. The table shows that 256 quantum states are obtained, which exactly corresponds to all possible combinations of 8 qubits, i.e.,  $2^8=256$  (counted from the far right of each state). The feasibility label qubit is the 9<sup>th</sup> qubit counted from the right. The labels of the states shown in the first 37 rows are 0, while those in rows 38-64 are 1. A label of 0 represents an infeasible solution, while a label of 1 indicates a feasible solution. Considering that each row has 4 states, there are 148 infeasible states and 108 feasible states, which matches the number calculated in the previous paragraph and validates the QFL.

## 5. Conclusion

In summary, we have successfully developed a QFL algorithm that provides a feasibility label for every possible solution to the vertex coloring problem. The QFL algorithm convert the vertex coloring problem into the problem of searching an unstructured database where good and bad elements are labeled with qubits  $|1\rangle$  and  $|0\rangle$ , respectively. The output of this algorithm can be directly input into the VQS algorithm, which can then find all feasible solutions. Notably, the computational complexity of the QFL is a polynomial function of the color options, vertices, and edges within a given vertex coloring problem.

We had numerically validated the efficiency of the VQS for cases involving up to 26 qubits in our previous work. The next critical milestone lies in extending this efficiency to all possible qubit numbers, which, if achieved, would mark a profound breakthrough. This achievement would signify that NP-complete problems can be efficiently addressed through the power of quantum algorithms.

Table 3. Measurement results. The strings in single quotes represent measured quantum states, and the number after a colon is the number of times that the state shown in the same cell is obtained from measurement.

row	State:count	State:count	State:count	State:count
1	'00000000000000': 86	'000000000000100': 80	'000000000000101': 64	'000000000001000': 83
2	'000000000001010': 83	'000000000001100': 84	'000000000001111': 72	'000000000010000': 69
3	'000000000010001': 69	'000000000010100': 68	'000000000010101': 93	'000000000011000': 71
4	'000000000011001': 77	'000000000011010': 69	'000000000011100': 80	'000000000011101': 65
5	'000000000011111': 78	'000000000010000': 86	'0000000000100010': 81	'000000000100100': 75
6	'000000000100101': 68	'000000000100110': 90	'000000000101000': 68	'000000000101010': 75
7	'000000000101100': 84	'000000000101110': 60	'000000000101111': 68	'000000000110000': 69
8	'000000000110011': 89	'000000000110100': 80	'000000000110101': 77	'000000000110111': 71
9	'000000000111000': 84	'000000000111010': 72	'000000000111011': 77	'000000000111100': 73
10	'000000000111111': 81	'000000000100000': 68	'000000000100001': 80	'000000000100010': 89
11	'0000000001000101': 90	'0000000001001000': 78	'0000000001001001': 81	'0000000001001010': 69
12	'0000000001001100': 85	'0000000001001101': 84	'0000000001001111': 75	'0000000001010000': 72
13	'0000000001010001': 72	'0000000001010101': 83	'0000000001011001': 70	'0000000001011010': 79
14	'0000000001011101': 76	'0000000001011111': 89	'0000000001100000': 88	'0000000001100001': 74
15	'0000000001100010': 67	'0000000001100101': 68	'0000000001100110': 74	'0000000001101001': 82
16	'0000000001101010': 65	'0000000001101101': 61	'0000000001101110': 84	'0000000001101111': 84
17	'0000000001110000': 87	'0000000001110001': 74	'0000000001110011': 72	'0000000001110101': 77
18	'0000000001110111': 81	'0000000001111001': 80	'0000000001111010': 76	'0000000001111011': 79
19	'0000000001111101': 94	'0000000001111111': 88	'0000000001000000': 86	'0000000001000010': 78
20	'0000000001000100': 79	'0000000001000101': 82	'0000000001000110': 88	'00000000010001000': 69
21	'00000000010001010': 67	'00000000010001100': 74	'00000000010001110': 78	'00000000010001111': 84
22	'00000000010010000': 87	'00000000010010001': 89	'00000000010010010': 89	'00000000010010101': 74
23	'00000000010010110': 63	'00000000010011001': 66	'00000000010011010': 75	'00000000010011101': 70
24	'00000000010011110': 80	'00000000010011111': 78	'00000000010100000': 66	'00000000010100010': 80

25	'0000000010100101': 89	'0000000010100110': 73	'0000000010101010': 81	'0000000010101110': 80
26	'0000000010101111': 73	'0000000010110000': 84	'0000000010110010': 69	'0000000010110011': 86
27	'0000000010110101': 83	'0000000010110110': 92	'0000000010110111': 73	'0000000010111010': 88
28	'0000000010111011': 73	'0000000010111110': 76	'0000000010111111': 83	'0000000011000000': 71
29	'0000000011000011': 86	'0000000011000100': 79	'0000000011000101': 75	'0000000011000111': 67
30	'0000000011001000': 80	'0000000011001010': 70	'0000000011001011': 89	'0000000011001100': 68
31	'0000000011001111': 71	'0000000011010000': 68	'0000000011010001': 84	'0000000011010011': 70
32	'0000000011010101': 80	'0000000011010111': 70	'0000000011011001': 93	'0000000011011010': 71
33	'0000000011011011': 84	'0000000011011101': 81	'0000000011011111': 67	'0000000011100000': 97
34	'0000000011100010': 83	'0000000011100011': 87	'0000000011100101': 73	'0000000011100110': 80
35	'0000000011100111': 86	'0000000011101010': 78	'0000000011101011': 70	'0000000011101110': 68
36	'0000000011101111': 63	'0000000011110000': 81	'0000000011110011': 68	'0000000011110101': 79
37	'0000000011110111': 72	'0000000011111010': 89	'0000000011111011': 87	'0000000011111111': 83
38	'000000010000001': 67	'000000010000010': 104	'000000010000011': 93	'000000010000110': 66
39	'000000010000111': 83	'0000000100001001': 66	'0000000100001011': 58	'0000000100001101': 66
40	'0000000100001110': 72	'0000000100010010': 77	'0000000100010011': 89	'0000000100010110': 91
41	'0000000100010111': 73	'0000000100011011': 66	'0000000100011110': 90	'0000000100100001': 92
42	'0000000100100011': 80	'0000000100100111': 78	'0000000100101001': 80	'0000000100101011': 82
43	'0000000100101101': 77	'0000000100110001': 70	'0000000100110010': 81	'0000000100110110': 73
44	'0000000100111001': 105	'0000000100111101': 84	'0000000100111110': 82	'0000000101000010': 69
45	'0000000101000011': 94	'0000000101000110': 74	'0000000101000111': 76	'0000000101001011': 84
46	'0000000101001110': 83	'0000000101010010': 83	'0000000101010011': 78	'0000000101010100': 65
47	'0000000101010110': 75	'0000000101010111': 86	'0000000101011000': 81	'0000000101011011': 64
48	'0000000101011100': 91	'0000000101011110': 79	'0000000101100011': 83	'0000000101100100': 77
49	'0000000101100111': 66	'0000000101101000': 82	'0000000101101011': 64	'0000000101101100': 79
50	'0000000101110010': 83	'0000000101110100': 77	'0000000101110110': 92	'0000000101111000': 83
51	'0000000101111100': 98	'0000000101111110': 86	'0000000110000001': 88	'0000000110000011': 88
52	'0000000110000111': 76	'0000000110001001': 78	'0000000110001011': 73	'0000000110001101': 87
53	'0000000110010011': 65	'0000000110010100': 80	'0000000110010111': 95	'0000000110011000': 84
54	'0000000110011011': 90	'0000000110011100': 68	'0000000110100001': 67	'0000000110100011': 71
55	'0000000110100100': 77	'0000000110100111': 78	'0000000110101000': 82	'0000000110101001': 87
56	'0000000110101011': 84	'0000000110101100': 71	'0000000110101101': 67	'0000000110110001': 86
57	'0000000110110100': 78	'0000000110111000': 76	'0000000110111001': 92	'0000000110111100': 82
58	'0000000110111101': 67	'0000000111000001': 70	'0000000111000010': 81	'0000000111000110': 100
59	'0000000111001001': 73	'0000000111001101': 69	'0000000111001110': 80	'0000000111010010': 75
60	'0000000111010100': 82	'0000000111010110': 72	'0000000111011000': 75	'0000000111011100': 76
61	'0000000111011110': 91	'0000000111100001': 72	'0000000111100100': 69	'0000000111101000': 74
62	'0000000111101001': 83	'0000000111101100': 69	'0000000111101101': 74	'0000000111110001': 78
63	'0000000111110010': 95	'0000000111110100': 80	'0000000111110110': 85	'0000000111111000': 66
64	'0000000111111001': 75	'0000000111111100': 59	'0000000111111101': 78	'0000000111111110': 78

## Acknowledgements

This research was partially supported by the NSF ERI program, under award number 2138702. The author acknowledges the use of IBM Quantum services for this work. The views expressed are those of the author, and do not reflect the official policy or position of IBM or the IBM Quantum team.

## Reference

- [1] S. Arora and B. Barak, *Computational Complexity: A Modern Approach*, Illustrated Edition., no. January. Cambridge University Press, 2009. doi: 10.1088/1742-6596/1/1/035.
- [2] M. Sipser, *Introduction to the Theory of Computation*, Second Edition., no. 9. 2006.
- [3] D. L. Applegate, R. E. Bixby, Vasek. Chvatal, and W. J. Cook, *The Traveling Salesman Problem : a Computational Study*. Princeton University Press, 2006.
- [4] S. Lin and B. W. Kernighan, “An Effective Heuristic Algorithm for the Traveling-Salesman Problem,” *Oper Res*, vol. 21, no. 2, pp. 498–516, Apr. 1973, doi: 10.1287/OPRE.21.2.498.

- [5] I. Khoufi, A. Laouiti, and C. Adjih, “A Survey of Recent Extended Variants of the Traveling Salesman and Vehicle Routing Problems for Unmanned Aerial Vehicles,” *Drones* 2019, Vol. 3, Page 66, vol. 3, no. 3, p. 66, Aug. 2019, doi: 10.3390/DRONES3030066.
- [6] S. Martello and P. Toth, *Knapsack Problems: Algorithms and Computer Implementations (Wiley Series in Discrete Mathematics and Optimization)*, 1st Edition. John Wiley & Sons, 1990. Accessed: Dec. 28, 2022. [Online]. Available: <https://www.amazon.com/Knapsack-Problems-Implementations-Mathematics-Optimization/dp/0471924202>
- [7] V. Cacchiani, M. Iori, A. Locatelli, and S. Martello, “Knapsack problems — An overview of recent advances. Part I: Single knapsack problems,” *Comput Oper Res*, vol. 143, p. 105692, Jul. 2022, doi: 10.1016/J.COR.2021.105692.
- [8] V. Cacchiani, M. Iori, A. Locatelli, and S. Martello, “Knapsack problems — An overview of recent advances. Part II: Multiple, multidimensional, and quadratic knapsack problems,” *Comput Oper Res*, vol. 143, p. 105693, Jul. 2022, doi: 10.1016/J.COR.2021.105693.
- [9] D. Pisinger, “The quadratic knapsack problem—a survey,” *Discrete Appl Math (1979)*, vol. 155, no. 5, pp. 623–648, Mar. 2007, doi: 10.1016/J.DAM.2006.08.007.
- [10] S. Malik and L. Zhang, “Boolean satisfiability from theoretical hardness to practical success,” *Commun ACM*, vol. 52, no. 8, pp. 76–82, Aug. 2009, doi: 10.1145/1536616.1536637.
- [11] A. Braunstein, M. Mézard, and R. Zecchina, “Survey propagation: an algorithm for satisfiability,” *Random Struct Algorithms*, vol. 27, no. 2, pp. 201–226, Dec. 2002, doi: 10.48550/arxiv.cs/0212002.
- [12] T. N. Alyahya, M. E. B. Menai, and H. Mathkour, “On the Structure of the Boolean Satisfiability Problem: A Survey,” *ACM Computing Surveys (CSUR)*, vol. 55, no. 3, pp. 1–34, Mar. 2022, doi: 10.1145/3491210.
- [13] L. Zhang, C. F. Madigan, M. H. Moskewicz, and S. Malik, “Efficient conflict driven learning in a boolean satisfiability solver,” *IEEE/ACM International Conference on Computer-Aided Design, Digest of Technical Papers*, pp. 279–285, 2001, doi: 10.1109/ICCAD.2001.968634.
- [14] M. W. Moskewicz, C. F. Madigan, Y. Zhao, L. Zhang, and S. Malik, “Chaff: engineering an efficient SAT solver,” *Proceedings of the 38th conference on Design automation - DAC '01*, pp. 530–535, 2001, doi: 10.1145/378239.379017.
- [15] D. L. Kreher and D. R. Stinson, *Combinatorial Algorithms: Generation, Enumeration, and Search (Discrete Mathematics and Its Applications)*, 1st Edition. CRC Press, 1998.
- [16] D. B. West, *Introduction to Graph Theory*, Second Edition. 2000.
- [17] C. H. Papadimitriou and K. Steiglitz, *Combinatorial Optimization: Algorithms and Complexity*. Courier Dover Publications, 1998.
- [18] F. Arute, K. Arya, R. Babbush, D. Bacon, J. C. Bardin, R. Barends, R. Biswas, S. Boixo, F. G. S. L. Brandao, D. A. Buell, B. Burkett, Y. Chen, Z. Chen, B. Chiaro, R. Collins, W. Courtney, A. Dunsworth, E. Farhi, B. Foxen, A. Fowler, C. Gidney, M. Giustina, R. Graff, K. Guerin, S. Habegger, M. P. Harrigan, M. J. Hartmann, A. Ho, M. Hoffmann, T. Huang, T. S. Humble, S. v. Isakov, E. Jeffrey, Z. Jiang, D. Kafri, K. Kechedzhi, J. Kelly, P. v. Klimov, S. Knysh, A. Korotkov, F. Kostritsa, D. Landhuis, M. Lindmark, E. Lucero, D. Lyakh, S. Mandrà, J. R. McClean, M. McEwen, A. Megrant, X. Mi, K. Michielsen, M. Mohseni, J. Mutus, O. Naaman, M. Neeley, C. Neill, M. Y. Niu, E. Ostby, A. Petukhov, J. C. Platt, C. Quintana, E. G. Rieffel, P. Roushan, N. C. Rubin, D. Sank, K.

- J. Satzinger, V. Smelyanskiy, K. J. Sung, M. D. Trevithick, A. Vainsencher, B. Villalonga, T. White, Z. J. Yao, P. Yeh, A. Zalcman, H. Neven, and J. M. Martinis, “Quantum supremacy using a programmable superconducting processor,” *Nature*, vol. 574, no. 7779, 2019, doi: 10.1038/s41586-019-1666-5.
- [19] A. W. Harrow, A. Hassidim, and S. Lloyd, “Quantum algorithm for linear systems of equations,” *Phys Rev Lett*, vol. 103, no. 15, 2009, doi: 10.1103/PhysRevLett.103.150502.
- [20] J.-P. Liu, H. Ø. Kolden, H. K. Krovi, N. F. Loureiro, K. Trivisa, and A. M. Childs, “Efficient quantum algorithm for dissipative nonlinear differential equations,” *arXiv:2011.03185*. 2021.
- [21] S. Lloyd, G. de Palma, C. Gokler, B. Kiani, Z.-W. Liu, M. Marvian, F. Tennie, and T. Palmer, “Quantum algorithm for nonlinear differential equations,” *arXiv:2011.06571*. 2020.
- [22] L. K. Grover, “Quantum mechanics helps in searching for a needle in a haystack,” *Phys Rev Lett*, vol. 79, no. 2, 1997, doi: 10.1103/PhysRevLett.79.325.
- [23] L. K. Grover, “A fast quantum mechanical algorithm for database search,” in *Proceedings of the Annual ACM Symposium on Theory of Computing*, 1996, vol. Part F129452. doi: 10.1145/237814.237866.
- [24] P. W. Shor, “Polynomial-time algorithms for prime factorization and discrete logarithms on a quantum computer,” *SIAM J. Comput.*, vol. 26, no. 5, pp. 1484–1509, 1997, doi: 10.1137/s0097539795293172.
- [25] G. Brassard, P. Høyer, M. Mosca, and A. Tapp, “Quantum amplitude amplification and estimation,” *Contemp. Math.*, vol. 305, pp. 53–74, 2002, doi: 10.1090/conm/305/05215.
- [26] Editorial, “Light on quantum advantage,” *Nature Materials 2021 20:3*, vol. 20, no. 3, pp. 273–273, Feb. 2021, doi: 10.1038/s41563-021-00953-0.
- [27] H. sen Zhong, H. Wang, Y. H. Deng, M. C. Chen, L. C. Peng, Y. H. Luo, J. Qin, D. Wu, X. Ding, Y. Hu, P. Hu, X. Y. Yang, W. J. Zhang, H. Li, Y. Li, X. Jiang, L. Gan, G. Yang, L. You, Z. Wang, L. Li, N. le Liu, C. Y. Lu, and J. W. Pan, “Quantum computational advantage using photons,” *Science (1979)*, vol. 370, no. 6523, pp. 1460–1463, Dec. 2020, doi: 10.1126/SCIENCE.ABE8770/SUPPL\_FILE/ABE8770\_ZHONG\_SM.PDF.
- [28] L. S. Madsen, F. Laudenbach, M. F. Askarani, F. Rortais, T. Vincent, J. F. F. Bulmer, F. M. Miatto, L. Neuhaus, L. G. Helt, M. J. Collins, A. E. Lita, T. Gerrits, S. W. Nam, V. D. Vaidya, M. Menotti, I. Dhand, Z. Vernon, N. Quesada, and J. Lavoie, “Quantum computational advantage with a programmable photonic processor,” *Nature 2022 606:7912*, vol. 606, no. 7912, pp. 75–81, Jun. 2022, doi: 10.1038/s41586-022-04725-x.
- [29] J. Zhan, “Variational Quantum Search with Shallow Depth for Unstructured Database Search,” Dec. 2022, Accessed: Oct. 08, 2023. [Online]. Available: <https://arxiv.org/abs/2212.09505v2>
- [30] J. M. Arrazola, V. Bergholm, K. Brádler, T. R. Bromley, M. J. Collins, I. Dhand, A. Fumagalli, T. Gerrits, A. Goussev, L. G. Helt, J. Hundal, T. Isacsson, R. B. Israel, J. Izaac, S. Jahangiri, R. Janik, N. Killoran, S. P. Kumar, J. Lavoie, A. E. Lita, D. H. Mahler, M. Menotti, B. Morrison, S. W. Nam, L. Neuhaus, H. Y. Qi, N. Quesada, A. Reppingon, K. K. Sabapathy, M. Schuld, D. Su, J. Swinarton, A. Száva, K. Tan, P. Tan, V. D. Vaidya, Z. Vernon, Z. Zabaneh, and Y. Zhang, “Quantum circuits with many photons on a programmable nanophotonic chip,” *Nature*, vol. 591, no. 7848, 2021, doi: 10.1038/s41586-021-03202-1.

- [31] N. W. Hendrickx, W. I. L. Lawrie, M. Russ, F. van Riggelen, S. L. de Snoo, R. N. Schouten, A. Sammak, G. Scappucci, and M. Veldhorst, “A four-qubit germanium quantum processor,” *Nature*, vol. 591, no. 7851, 2021, doi: 10.1038/s41586-021-03332-6.
- [32] A. Peruzzo, J. McClean, P. Shadbolt, M. H. Yung, X. Q. Zhou, P. J. Love, A. Aspuru-Guzik, and J. L. O’Brien, “A variational eigenvalue solver on a photonic quantum processor,” *Nat Commun*, vol. 5, 2014, doi: 10.1038/ncomms5213.
- [33] E. Hyppä, S. Kundu, C. F. Chan, A. Gunyhó, J. Hotari, D. Janzso, K. Juliusson, O. Kiuru, J. Kotilahti, A. Landra, W. Liu, F. Marxer, A. Mäkinen, J.-L. Orgiazzi, M. Palma, M. Savytskyi, F. Tosto, J. Tuorila, V. Vadimov, T. Li, C. Ockeloen-Korppi, J. Heinsoo, K. Y. Tan, J. Hassel, M. Möttönen, Y. Kuan, J. Tan, and M. M. Hassel, “Unimon qubit,” *Nat Commun*, vol. 13, no. 1, pp. 1–14, Nov. 2022, doi: 10.1038/s41467-022-34614-w.
- [34] IBM Quantum, “<https://quantum-computing.ibm.com/>,” 2021, Accessed: Jun. 11, 2021. [Online]. Available: <https://quantum-computing.ibm.com/>
- [35] Rigetti, “Rigetti.” <https://www.rigetti.com/> (accessed Dec. 28, 2022).
- [36] Amazon, “Amazon Braket.” <https://aws.amazon.com/braket/> (accessed Dec. 28, 2022).
- [37] IBM, “IBM Quantum Roadmap,” <https://research.ibm.com/blog/ibm-quantum-roadmap-2025>.
- [38] J. Gambetta, “IBM’s Roadmap For Scaling Quantum Technology,” Sep. 15, 2020. <https://www.ibm.com/blogs/research/2020/09/ibm-quantum-roadmap/> (accessed Jun. 11, 2021).
- [39] V. Bergholm, J. Izaac, M. Schuld, C. Gogolin, S. Ahmed, V. Ajith, M. S. Alam, G. Alonso-Linaje, B. AkashNarayanan, A. Asadi, J. M. Arrazola, U. Azad, S. Banning, C. Blank, T. R. Bromley, B. A. Cordier, J. Ceroni, A. Delgado, O. di Matteo, A. Dusko, T. Garg, D. Guala, A. Hayes, R. Hill, A. Ijaz, T. Isacsson, D. Ittah, S. Jahangiri, P. Jain, E. Jiang, A. Khandelwal, K. Kottmann, R. A. Lang, C. Lee, T. Loke, A. Lowe, K. McKiernan, J. J. Meyer, J. A. Montañez-Barrera, R. Moyard, Z. Niu, L. J. O’Riordan, S. Oud, A. Panigrahi, C.-Y. Park, D. Polatajko, N. Quesada, C. Roberts, N. Sá, I. Schoch, B. Shi, S. Shu, S. Sim, A. Singh, I. Strandberg, J. Soni, A. Száva, S. Thabet, R. A. Vargas-Hernández, T. Vincent, N. Vitucci, M. Weber, D. Wierichs, R. Wiersema, M. Willmann, V. Wong, S. Zhang, and N. Killoran, “PennyLane: Automatic differentiation of hybrid quantum-classical computations.” arXiv, 2018. doi: 10.48550/ARXIV.1811.04968.
- [40] N. Wiebe, D. Braun, and S. Lloyd, “Quantum algorithm for data fitting,” *Phys. Rev. Lett.*, vol. 109, no. 5, p. 050505, Aug. 2012, doi: 10.1103/physrevlett.109.050505.
- [41] P. Rebentrost, M. Mohseni, and S. Lloyd, “Quantum support vector machine for big data classification,” *Phys. Rev. Lett.*, vol. 113, no. 3, p. 130503, Sep. 2014, doi: 10.1103/physrevlett.113.130503.
- [42] J. Biamonte, P. Wittek, N. Pancotti, P. Rebentrost, N. Wiebe, and S. Lloyd, “Quantum machine learning,” *Nature*, vol. 549, no. 7671. Nature Publishing Group, pp. 195–202, Sep. 13, 2017. doi: 10.1038/nature23474.
- [43] S. Jordan, “Quantum Algorithm Zoo.” <https://quantumalgorithmzoo.org/> (accessed Jun. 13, 2021).
- [44] A. Montanaro, “Quantum algorithms: An overview,” *npj Quantum Information*, vol. 2, no. 1. 2016. doi: 10.1038/npjqi.2015.23.
- [45] A. M. Childs, R. Cleve, E. Deotto, E. Farhi, S. Gutmann, and D. A. Spielman, “Exponential algorithmic speedup by quantum walk,” p. 59, Sep. 2002, doi: 10.1145/780542.780552.

- [46] A. M. Childs, “Quantum algorithms: Equation solving by simulation,” *Nature Phys.*, vol. 5, no. 12, p. 861, 2009, doi: 10.1038/nphys1473.
- [47] B. D. Clader, B. C. Jacobs, and C. R. Sprouse, “Preconditioned quantum linear system algorithm,” *Phys.Rev. Lett.*, vol. 110, no. 25, p. 250504, Jun. 2013, doi: 10.1103/physrevlett.110.250504.
- [48] A. J., A. Adedoyin, J. Ambrosiano, P. Anisimov, A. Bärtschi, W. Casper, G. Chennupati, C. Coffrin, H. Djidjev, D. Gunter, S. Karra, N. Lemons, S. Lin, A. Malyzhenkov, D. Mascarenas, S. Mniszewski, B. Nadiga, D. O’Malley, D. Oyen, S. Pakin, L. Prasad, R. Roberts, P. Romero, N. Santhi, N. Sinitsyn, P. J. Swart, J. G. Wendelberger, B. Yoon, R. Zamora, W. Zhu, S. Eidenbenz, P. J. Coles, M. Vuffray, and A. Y. Lokhov, “Quantum Algorithm Implementations for Beginners,” *arXiv:1804.03719*. 2020.
- [49] K. Bharti, A. Cervera-Lierta, T. H. Kyaw, T. Haug, S. Alperin-Lea, A. Anand, M. Degroote, H. Heimonen, J. S. Kottmann, T. Menke, W.-K. Mok, S. Sim, L.-C. Kwek, and A. Aspuru-Guzik, “Noisy intermediate-scale quantum (NISQ) algorithms,” *arXiv:2101.08448*. 2021.
- [50] M. Cerezo, A. Arrasmith, R. Babbush, S. C. Benjamin, S. Endo, K. Fujii, J. R. McClean, K. Mitarai, X. Yuan, L. Cincio, and P. J. Coles, “Variational quantum algorithms,” *Nature Reviews Physics*, vol. 3, no. 9. Springer Nature, pp. 625–644, Sep. 01, 2021. doi: 10.1038/s42254-021-00348-9.
- [51] J. R. McClean, J. Romero, R. Babbush, and A. Aspuru-Guzik, “The theory of variational hybrid quantum-classical algorithms,” *New J Phys*, vol. 18, no. 2, 2016, doi: 10.1088/1367-2630/18/2/023023.
- [52] J. Tilly, H. Chen, S. Cao, D. Picozzi, K. Setia, Y. Li, E. Grant, L. Wossnig, I. Rungger, G. H. Booth, and J. Tennyson, “The Variational Quantum Eigensolver: A review of methods and best practices,” *Phys Rep*, vol. 986, pp. 1–128, Nov. 2022, doi: 10.1016/j.physrep.2022.08.003.
- [53] E. Farhi and A. W. Harrow, “Quantum Supremacy through the Quantum Approximate Optimization Algorithm.” *arXiv*, 2016. doi: 10.48550/ARXIV.1602.07674.
- [54] C. Bravo-Prieto, R. LaRose, M. Cerezo, Y. Subasi, L. Cincio, and P. J. Coles, “Variational Quantum Linear Solver.” *arXiv*, 2019. doi: 10.48550/ARXIV.1909.05820.
- [55] N. Moll, P. Barkoutsos, L. S. Bishop, J. M. Chow, A. Cross, D. J. Egger, S. Filipp, A. Fuhrer, J. M. Gambetta, M. Ganzhorn, A. Kandala, A. Mezzacapo, P. Müller, W. Riess, G. Salis, J. Smolin, I. Tavernelli, and K. Temme, “Quantum optimization using variational algorithms on near-term quantum devices,” *Quantum Sci Technol*, vol. 3, no. 3, p. 030503, Jun. 2018, doi: 10.1088/2058-9565/AAB822.
- [56] S. McArdle, T. Jones, S. Endo, Y. Li, S. C. Benjamin, and X. Yuan, “Variational ansatz-based quantum simulation of imaginary time evolution,” *npj Quantum Inf*, vol. 5, no. 1, 2019, doi: 10.1038/s41534-019-0187-2.
- [57] K. Mitarai, Y. O. Nakagawa, and W. Mizukami, “Theory of analytical energy derivatives for the variational quantum eigensolver,” *Phys Rev Res*, vol. 2, no. 1, Feb. 2020, doi: 10.1103/physrevresearch.2.013129.
- [58] R. A. Bravo, K. Najafi, T. L. Patti, X. Gao, and S. F. Yelin, “Universal Quantum Perceptrons for Quantum Machine Learning,” Nov. 2022, doi: 10.48550/arxiv.2211.07075.
- [59] W. Huggins, P. Patil, B. Mitchell, K. Birgitta Whaley, and E. Miles Stoudenmire, “Towards quantum machine learning with tensor networks,” *Quantum Sci Technol*, vol. 4, no. 2, 2019, doi: 10.1088/2058-9565/aaea94.

- [60] A. Skolik, J. R. McClean, M. Mohseni, P. van der Smagt, and M. Leib, “Layerwise learning for quantum neural networks,” *Quantum Mach Intell*, vol. 3, no. 1, 2021, doi: 10.1007/s42484-020-00036-4.
- [61] Y. Liao and J. Zhan, “Expressibility-Enhancing Strategies for Quantum Neural Networks,” Nov. 2022, Accessed: Dec. 21, 2022. [Online]. Available: <https://arxiv.org/abs/2211.12670v1>
- [62] S. Lloyd, M. Mohseni, and P. Rebentrost, “Quantum principal component analysis,” *Nature Phys.*, vol. 10, no. 9, pp. 631–633, 2014, doi: 10.1038/nphys3029.
- [63] K. Mitarai, M. Negoro, M. Kitagawa, and K. Fujii, “Quantum circuit learning,” *Phys Rev A (Coll Park)*, vol. 98, no. 3, 2018, doi: 10.1103/PhysRevA.98.032309.
- [64] S. Aaronson, “Guest Column: NP-complete problems and physical reality,” *ACM SIGACT News*, vol. 36, no. 1, 2005, doi: 10.1145/1052796.1052804.
- [65] S. Aaronson, A. Bouland, J. Fitzsimons, and M. Lee, “The Space ‘just above’ BQP,” 2016. doi: 10.1145/2840728.2840739.
- [66] K. Shimizu and R. Mori, “Exponential-Time Quantum Algorithms for Graph Coloring Problems,” *Algorithmica*, vol. 84, no. 12, pp. 3603–3621, Dec. 2022, doi: 10.1007/S00453-022-00976-2/TABLES/3.
- [67] M. Fürer, “Solving NP-complete problems with quantum search,” *Lecture Notes in Computer Science (including subseries Lecture Notes in Artificial Intelligence and Lecture Notes in Bioinformatics)*, vol. 4957 LNCS, pp. 784–792, 2008, doi: 10.1007/978-3-540-78773-0\_67/COVER.
- [68] A. N. Nagamani, S. Ashwin, and V. K. Agrawal, “Design of optimized reversible binary adder/subtractor and BCD adder,” *Proceedings of 2014 International Conference on Contemporary Computing and Informatics, IC3I 2014*, pp. 774–779, Jan. 2014, doi: 10.1109/IC3I.2014.7019664.